A Different Perspective on the Export of Water from the South Atlantic

DORON NOF* AND STEPHEN VAN GORDER

Department of Oceanography, The Florida State University, Tallahassee, Florida

(Manuscript received 26 June 1998, in final form 19 October 1998)

ABSTRACT

A different way of looking at the meridional warm water ($\sigma_\theta < 26.8$) flux in the South and North Atlantic is proposed. The approach involves the blending of observational aspects into analytical modeling, which allows one to circumvent finding a detailed solution to the complete wind–thermohaline problem. The method employs an integration of the momentum equations along a ''horseshoe'' path in a rectangular basin that is open on the southern side.

The initial model considered involves a northward flowing upper layer, a stagnant intermediate layer, and a southward flowing deep layer. By choosing the integration path to begin at one separation point (the Brazil Current separation from South America) and end at another separation point (the Gulf Stream separation), a rather simple expression for the meridional upper-layer transport (T) is obtained. In this scenario the high-latitude cooling affects the warm water northward transport through its influence on the latitude of the western boundary current separation.

The authors find that the combined transport (i.e., the transport induced by both wind and high-latitude cooling) is given by $T = \int (\tau^l/\rho)\, dl/(f_1 - f_2)$, where f_1 and f_2 are the Coriolis parameters along the northern and southern separation latitudes (i.e., $f_2 < 0$), and τ^l is the wind stress along the integration path (l). The amount of high-latitude cooling that causes the deep-water formation in the North Atlantic does not enter this relationship explicitly but it does enter the calculations implicitly (through the position of the separation points that adjust to the cooling). Process-oriented numerical experiments, which were conducted using MICOM, are in excellent agreement with the above formula.

Surprisingly, application of the formula to the Atlantic gives a transport of less than one Sverdrup (Sv $\equiv 10^6$ m^3 s^{-1}), an amount that is insignificant compared to the frequently quoted values (10–20 Sv). This questions the common suggestion that surface Atlantic Water flows northward and sinks in high latitude due to wind and high-latitude cooling *alone.* The difficulty is resolved when a *low* or *midlatitude* conversion of Atlantic Intermediate Water to upper thermocline water (via upwelling) is added (à la Goldsbrough) to the model. This implies that the upwelling needed to balance the deep-water formation in the North Atlantic must occur within the limits of the Atlantic Ocean itself rather than in the Pacific and the Indian Oceans. An additional point of interest is that the inclusion of upwelling does not show that all the upwelled water ultimately sinks in the North Atlantic. Rather, it shows that any amount of upwelled intermediate water (at low and midlatitudes) must be *equally split* between a flow that exits the northern gyre on the north side and a flow that exits the South Atlantic somewhere along the section connecting the mean position of the Brazil Current separation point and the tip of South Africa.

1. Introduction

Determination of the meridional mass flux in the ocean is important because of its direct relevance to the earth's climate. Traditionally, this transport has been viewed as consisting of two distinctly separate parts, the thermohaline circulation (driven by density differences resulting from heat exchange with the atmosphere or freshwater input and output) and the wind-driven circulation. In reality, the two kinds of circulation may not always be separated and our present problem represents such a case.

We shall consider the question of how much water flows northward from the South Atlantic (and ultimately sinks in the North Atlantic) in terms of a wind-driven intergyre exchange process coupled with high-latitude cooling. Our approach is different than that usually taken in that it involves a mixture of analytical modeling and observations. Specifically, we shall consider analytical models and, instead of solving the (incredibly complicated) complete wind–thermohaline problem, we shall blend into the analytical models the observed position of western boundary current (WBC) separation. This blending of the separation latitudes will essentially eliminate the *explicit* appearance of thermohaline pro-

* Additional affiliation: Geophysical Fluid Dynamics Institute, The Florida State University, Tallahassee, Florida

Corresponding author address: Dr. Doron Nof, Department of Oceanography (4320), The Florida State University, Tallahassee, FL 32306-4320.
E-mail: nof@ocean.fsu.edu

cesses in the problem but retain their implicit appearance (through the position of the WBC separation).

Surface cooling is assumed to take place only in high latitudes and, with our particular approach, it will enter the problem indirectly through the position of the WBC separation. We shall see that any kind of intergyre exchange bounded from the southwest and northwest by two separating boundary currents (i.e., the Brazil Current and the Gulf Stream) must involve some sort of *asymmetry* in the wind field, the land distribution, or the high-latitude cooling. Furthermore, we shall see that, in the Atlantic, this asymmetry is insignificant in the sense that the observed high-latitude cooling, the wind pattern, and the distribution of the continents allow for only a very small amount of warm water ($\sigma_\theta < 26.8$) to be transported northward. This suggests that what are usually thought to be the main driving forces of the overturning cell (wind and high-latitude cooling) are not sufficient to drive the observed northward transport. It turns out that, as other studies suggested, *low* and *midlatitude* upwelling is essential for the northward transport to take place. However, the process does not involve simple upwelling and sinking. It turns out that when low and midlatitude upwelling into the thermocline is added to the model, about 10–20 Sv (Sv $\equiv 10^6$ m^3 s^{-1}) reach the high-latitude regions in the North Atlantic, but, surprisingly, an equal amount of upwelled water must flow southward and exit the South Atlantic (via the surface water).

a. Background

On the basis of water property analysis, Gordon (1986) was the first to suggest that the water that ultimately sinks in the North Atlantic enters the upper South Atlantic near the tip of South Africa. He suggested that warm water enters the South Atlantic mostly due to the influx of Agulhas rings. These rings are relatively large (~500 km in diameter) and deep (~800 m) and have been observed to drift westward at rates of 5–8 cm s^{-1} (Olson and Evans 1986).

Using inverse calculations, Rintoul (1991) disputed Gordon's (1986) arguments and suggested that the origin of the Atlantic water that ultimately sinks in the North Atlantic is the Drake Passage rather than the tip of South Africa (suggested by Gordon). He suggests that this cold water route accounts for roughly 17 Sv, which is equally split among surface, intermediate, and bottom water. In a subsequent article, Gordon et al. (1992) proposed a circulation pattern that is somewhat different from both Gordon's (1986) original suggestion and Rintoul's (1991) flow pattern. In their new scenario, much of the Indian Ocean surface water that enters the South Atlantic (via the Benguela Current and Agulhas rings) recirculates and exits the South Atlantic. Furthermore, the 10 Sv or so that, in their opinion, does cross the Atlantic equator consists mainly of intermediate rather than surface water. According to Gordon et al. (1992) this intermediate water originates in the Drake Passage and loops in the Indian Ocean before entering the Atlantic.

Saunders and King (1995) have used recent World Ocean Circulation Experiment data to argue that, as originally suggested by Gordon (1986), about 10 Sv of mainly surface water enters the South Atlantic along the warm water path. Schmitz (1996) also suggests such a warm water route. Recent numerical computations (Barnier et al. 1998; Marchesiello et al. 1998) suggest, on the other hand, that the overturning cell consists mainly of cold, rather than warm, water. These numerical calculations point to a transport of 16 Sv, which is in agreement with the recent hydrographic estimates of Schlitzer (1996). They are also consistent with Matano and Philander's (1993) calculations showing a conversion of intermediate to surface water in the South Atlantic. The reader is also referred to Drijfhout et al. (1996) where other aspects of this circulation are discussed. The reader is warned, however, that these model studies do not add much information to the above issue since they drive their overturning via their boundary conditions or choose (implicitly or explicitly) a mixing parameterization that determines overtuning.

Our new analytical technique will show that ''pure'' thermocline water (i.e., thermocline water that has not entrained any intermediate water) can be forced northward across the equator only if there are significant interhemispheric asymmetries in the wind field, the geography, or the high-latitude cooling. It turns out that the asymmetry in the shape of the continents surrounding the Atlantic, the observed wind field above the Atlantic, and the known high-latitude cooling are not sufficient to allow for a significant amount of warm water to be transported meridionally. Adding upwelling [à la Goldsbrough (1933)] to our model resolves this difficulty and shows that a conversion of intermediate water to thermocline water permits a significant northward flow. As mentioned, however, it also shows that the upwelled water must be equally split between the Northern and Southern Hemispheres.

b. Present approach

Consider first the idealized ''reduced gravity'' ocean shown in Figs. 1 and 2. This simplified configuration is sufficient for illustrating the essence of the problem and is used here merely for the clarity of the presentation. Actual calculations will be done with a more realistic continuously stratified ocean and more realistic geography (Fig. 3). We shall consider the familiar vertically integrated equations of motion corresponding to an ocean whose interior is wind driven and obeys Sverdrup dynamics (section 2). Dissipation occurs underneath the swift WBC as a result of interfacial friction. Cross-equatorial flow occurs via the WBC where the relative vorticity created by the meridional displacement of the fluid is immediately destroyed via friction. Some

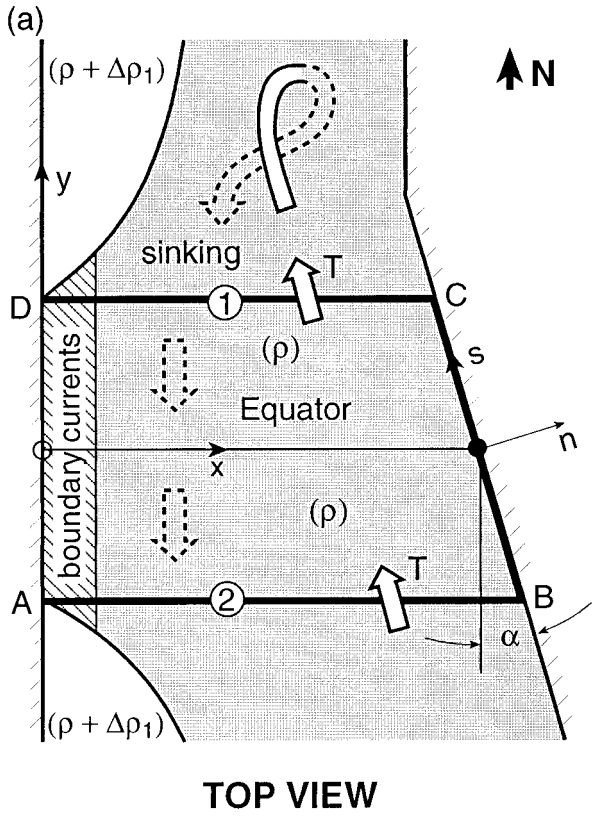

FIG. 1a. Schematic top view of the simplified meridional flow model. In this simplified version, which is used merely for the clarity of the presentation, the upper layer (shaded region corresponding to $\sigma_\theta < 26.8$) is driven northward by zonal winds and thermohaline processes. The upper water sinks outside the integration area and returns southward as a deep current (with a density $\rho + \Delta\rho_2$). An inert intermediate layer (with a density $\rho + \Delta\rho_1$) is sandwiched between the northward flowing surface water (thick open arrows) and the southward flowing deep water (thick broken arrows). Actual calculations for the Atlantic were done using a more realistic model, which takes into account the appropriate geography of the continents, the sphericity of the earth, meridional winds, and a continuous stratification within the upper water lens. Two coordinate systems will be used. The x and y system with x pointing eastward and y pointing northward will be used to describe the field equations; the n and s system with n normal to the eastern boundary and s along that boundary will be used to describe the boundary conditions along the eastern boundary. The thick line **ABCD** denotes the ''horseshoe'' integration path.

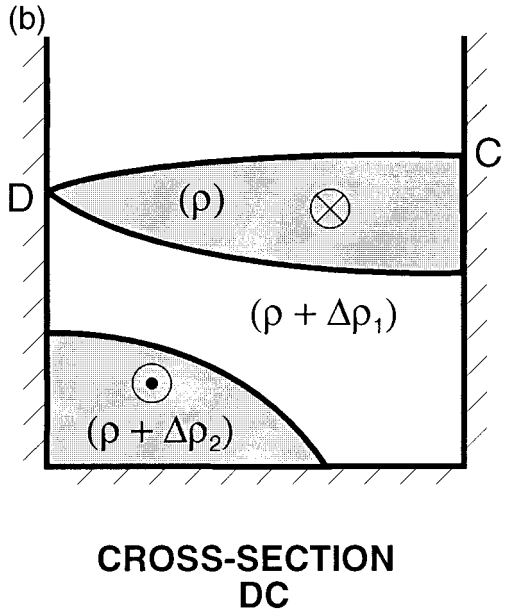

FIG. 1b. A cross section of the model shown in Fig. 1a.

nonlinearity is contained in the model through the pressure terms, but the inertial terms are neglected and the problem is linear in terms of the square of the layer thickness.

The common demand that, in a closed basin, the WBC transport be equal and opposite to that of the interior is relaxed so that a net meridional flow out of the region of interest is allowed. Such a net transport is, in general, a result of a combined interior and WBC fluxes. With the aid of these considerations and an integration along a ''horseshoe'' path connecting the two separation latitudes in both hemispheres, we shall analytically derive a formula that allows the computation of the meridional interhemispheric transport from the wind field and the WBC separation latitude. This meridional transport includes flows due to both wind and high-latitude diabatic processes. Integration of the governing equations across

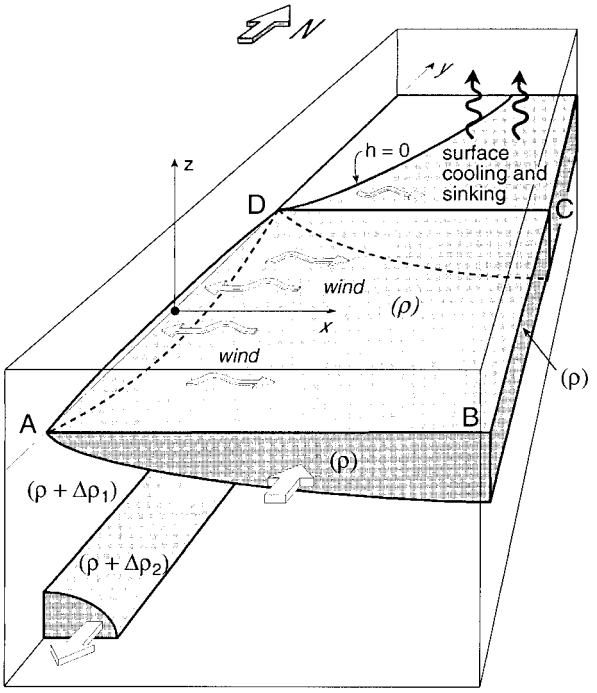

FIG. 2. A three-dimensional view of the model shown in Figs. 1a and 1b. Open ''wiggly'' arrows denote wind, open straight arrows denote transports, and solid wiggly arrows denote the cooling. Note that, in this model, cooling takes place in latitudes higher than the separation latitude (**DC**).

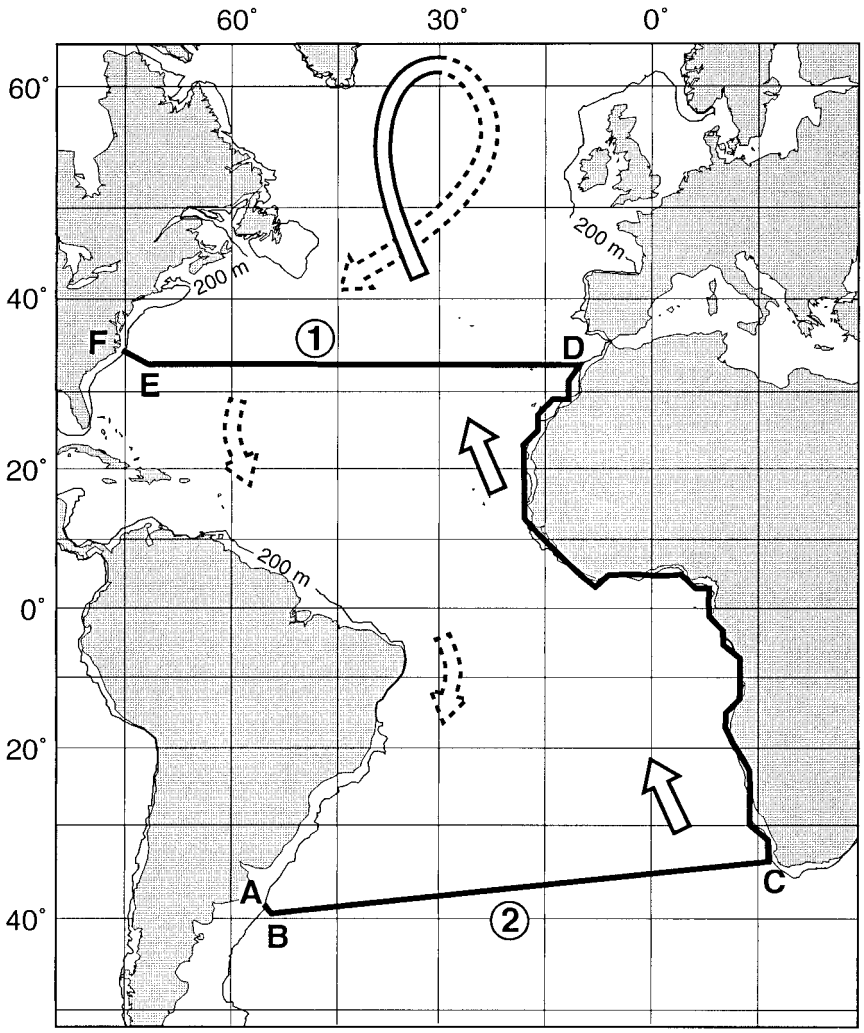

FIG. 3. A diagram of the horseshoe integration path used in the ''realistic'' model. Across the ocean (sections **BC** and **ED**) the integration is done mainly in the zonal direction; along the eastern boundary (**CD**) the coastline is followed. The western boundary is open save for integration across the boundary currents (**AB** and **EF**), which is done in the direction perpendicular to the coast. Points **F** and **A**, the mean positions of the separation points, were determined from Levitus climatological data by considering the intersection of the $\sigma_\theta = 26.8$ isopycnal with the coast at a depth of 100 m.

the ocean is, of course, not new and was considered earlier by various authors such as Parsons (1969) and Veronis (1973). What is new is the choice of our particular integration path (from one separation point to another), the calculation of the pressure differences along the boundaries which, surprisingly, allows us to entirely eliminate the pressure terms, and the recognition that high-latitude cooling processes can only enter the problem through the position of the WBC separation.

As already stated, in our calculations, cooling and sinking of thermocline water is assumed to occur in high latitudes beyond the separation latitude. In reality, there is some cooling equatorward of the separation latitude but most of the heat exchange does occur in the high-latitude regions as assumed here (see, e.g., Oberhuber 1988). We shall see that, even though cooling does not enter the model explicitly, it does enter the calculations implicitly through the position of the separation points, which adjust to the cooling.

After presenting the formula for the simple high-latitude cooling model and illustrating the essence of the problem (section 2), we shall proceed and extend the transport formula to the more realistic ocean shown in Fig. 3 (section 3). In this context, we shall include (i) a continuously stratified upper ocean rather than an upper layer with uniform densities (employed in the simple model), (ii) meridional winds, (iii) the sphericity of the earth, (iv) the actual geometry of the ocean boundaries, and (v) low and midlatitude upwelling. This is followed by presenting process-oriented numerical experiments (section 4) and com-

paring them to our transport formula. Some discussion of the results is included throughout the presentation; the application to the Atlantic is presented in detail in section 5 and a summary is given in section 6.

The above approach is an extension of Nof's (1998) recent derivation of the ''separation formula'' and its application to the Pacific Ocean and the Indonesian Throughflow. The main differences between the case considered here (i.e., the Atlantic) and that considered in Nof (1998) are (i) there is no deep-water formation in the Pacific and (ii) the Indonesian Passages are situated well to the south of the Kuroshio separation so that there is no net meridional flow in most of the Pacific Northern Hemisphere. As a result of these differences, the transport formulas are not at all the same in the two oceans. An additional difference between the two studies is that, by conducting a series of numerical experiments using the Bleck and Boudra isopycnic model, we carry here the ''separation formula'' a step further than in Nof (1998). We shall demonstrate that the formula's application to the Atlantic is in excellent agreement with the numerics. Note that there is some limited (unavoidable) overlap between the Nof (1998) article and the present one because an attempt has been made to make the present article self-contained. The overlap is limited to parts of section 2.

2. Derivation of the transport for the Atlantic Ocean

a. Governing equations

Consider again the model shown in Fig. 1. Following Nof (1998), we shall use the familiar vertically integrated equations of motion for the upper layer,

$$-fV = -\frac{1}{2}g'\frac{\partial}{\partial x}(h^2) + \frac{\tau^x}{\rho} \tag{2.1}$$

$$fU = -\frac{1}{2}g'\frac{\partial}{\partial y}(h^2) - RV \tag{2.2}$$

$$U_x + V_y = 0, \tag{2.3}$$

where h is the upper-layer thickness, U and V are the vertically integrated transports in the x and y direction (here x is pointing eastward and y northward), f is the Coriolis parameter (varying linearly with y), g' the ''reduced gravity'' $g\Delta\rho_1/\rho$ (where $\Delta\rho_1$ is the density difference between the upper and the intermediate layer and ρ is the density of the upper layer), τ^x the wind stress in the x direction, and R is an interfacial friction coefficient which need not be specified for the purpose of our analysis. The thick intermediate layer velocities are taken to be, on average, small compared to those of the upper layer. The equations are valid for all latitudes equatorward of sections **DC** and **AB** (Fig. 2) including the equator. As mentioned, the model excludes diabatic processes equatorward of the separation latitudes but does not exclude such processes poleward of the separation latitudes (which enter the problem through the position of the WBC separation).

Elimination of the pressure terms between (2.1) and (2.2) and consideration of (2.3) gives

$$\beta V = -\frac{1}{\rho}\frac{\partial \tau^x}{\partial y} - R\frac{\partial V}{\partial x}, \tag{2.4}$$

which, for the inviscid ocean interior, reduces to the familiar Sverdrup relationship,

$$\beta V = -\frac{1}{\rho}\frac{\partial \tau^x}{\partial y}. \tag{2.5}$$

Four comments should be made with regard to (2.1)–(2.5). First, in this model, energy is supplied by the wind over the entire ocean and is dissipated through interfacial friction [i.e., the RV term in (2.2)] within the limits of the WBC system. This interfacial friction is not present in (2.1) because RU is small and negligible. Furthermore, since the velocities are small in the ocean interior, the frictional term is negligible there.

Second, (2.1) holds both in the sluggish interior away from the boundaries and in the intense WBC where the flow is geostrophic in the cross-stream direction. Within the WBC the balance is between the Coriolis and pressure terms with the wind stress playing a secondary role. In the interior, on the other hand, the velocities are small and, consequently, all three terms are of the same order. Third, the inertial terms are excluded from the model but, to allow the interface to surface, nonlinearity is included in the pressure terms (via the square of the thickness). Since the model does not include relative vorticity within the WBC, it implicitly assumes that all relative vorticity generated by moving the fluid meridionally (within the boundary layer) is dissipated immediately after its creation. This implies that cross-equatorial flows can easily take place via the WBC where the fluid does not ''remember'' its origin.

Fourth, in this model, the frictional coefficient determines the width of the (unseparated) WBC but not its length (which, in turn, is controlled by the wind field and the thickness along the eastern boundary). In other words, the WBC adjusts its width in such a way that the total energy input (by the wind) is always dissipated along its base. Also, since in the interior the meridional transport is determined directly from the wind field (2.5), the total net meridional transport across the ocean is determined by the WBC.

Finally, it is perhaps appropriate to comment on the assumption of an inert intermediate layer because this assumption is frequently misunderstood. In contrast to common statements, the assumption does not imply negligible transports in the intermediate layer. It merely implies that the horizontal *pressure gradients* in the thick intermediate layer are small compared to the horizontal pressure gradients in the upper layer. This means that, on average, the speeds in the lower layer are small compared to the speeds in the upper layer; since the

intermediate layer thickness is much greater than the upper-layer thickness, the transports in the intermediate layer can be of the *same order* as those of the upper layer. Furthermore, since Ekman flows do not necessarily involve horizontal pressure gradients, they are not necessarily excluded from the intermediate layer.

b. Boundary conditions

The boundary condition along the solid boundaries is, of course, the familiar no-normal flow into the western and eastern walls. As in Nof (1998), it is convenient to use a tilted coordinate system n and s where n is normal to the eastern boundary and s is along the boundary. In terms of this tilted coordinate system, (2.1) and (2.3) (with the frictional term neglected) are

$$-[f_0 + \beta(s\cos\alpha + n\sin\alpha)]V = -\frac{g'}{2}\frac{\partial}{\partial n}(h^2) + \tau^x\frac{\cos\alpha}{\rho} \tag{2.6}$$

$$[f_0 + \beta(s\cos\alpha + n\sin\alpha)]U = -\frac{g'}{2}\frac{\partial}{\partial s}(h^2) + \tau^x\frac{\sin\alpha}{\rho}, \tag{2.7}$$

where α is the tilt of the boundary measured from the meridian (see Fig. 1), and U and V are now the integrated transports in the n and s directions.

Since $U \equiv 0$ along the boundary ($n = 0$) it follows immediately from (2.7) that

$$\frac{g'}{2}[h_{\mathbf{C}}^2 - h_{\mathbf{B}}^2] = \frac{1}{\rho}\int_{\mathbf{B}}^{\mathbf{C}} \tau^x \sin\alpha\, ds, \tag{2.8}$$

where $h_{\mathbf{C}}$ and $h_{\mathbf{B}}$ are the upper-layer thicknesses at **C** and **B**, respectively. Relation (2.8) implies that along the eastern coast the sea level responds to the wind stress in the usual wind setup manner (i.e., in the same manner that it would in a long and narrow lake). For a purely meridional boundary ($\alpha = 0$), (2.8) reduces to the familiar condition of constant depth along the eastern boundary (i.e., $h_{\mathbf{C}} = h_{\mathbf{B}}$) as should be the case. This completes our discussion of the eastern boundary condition.

As mentioned, along the western boundary the zonal velocity component also vanishes. However, in contrast to the eastern boundary, the thickness is not uniform along this boundary due to the frictional term. Nevertheless, there is an additional boundary condition that is crucial to our computation. It is the condition that both the southern and northern boundary currents separate from the coast at some points (**A** and **D**). This means that

$$h_{\mathbf{D}} = h_{\mathbf{A}} = 0, \tag{2.9}$$

where, as before, the subscripts **D** and **A** denote that the variable in question is associated with points **D** and **A** (see Fig. 1). Strictly speaking from a geophysical fluid dynamics point of view, the location of the separation points must be determined as a part of the solution to the wind and heat exchange problem. As mentioned, however, we take here a different approach and use the available observational information regarding the position of the separation as an input to our model. This, together with the (reasonable) choice of cooling poleward of the WBC separation latitude, but no cooling south of the separation latitude, essentially eliminates the explicit appearance of thermohaline processes in the mathematical problem. Thermohaline processes are, of course, an integral part of the problem at hand but, for cooling processes active only in high latitudes, they enter the problem only through their influence on the position of the WBC separation. We shall return to this important point later.

c. Integration of the momentum equation

To derive the transport formula, we follow Nof (1998) and integrate (2.1) from the western to the eastern boundary along the separation latitudes (i.e., sections 1 and 2 shown in Fig. 1),

$$f_1 T = \frac{g'}{2}\int_{\mathbf{D}}^{\mathbf{C}} \frac{\partial}{\partial x}(h^2)\, dx - \int_{\mathbf{D}}^{\mathbf{C}} \left(\frac{\tau^x}{\rho}\right) dx \tag{2.10a}$$

$$f_2 T = \frac{g'}{2}\int_{\mathbf{A}}^{\mathbf{B}} \frac{\partial}{\partial x}(h^2)\, dx - \int_{\mathbf{A}}^{\mathbf{B}} \frac{\tau^x}{\rho}\, dx, \tag{2.10b}$$

where T is the net meridional transport across the ocean and f_1 and f_2 are the Coriolis parameters along sections 1 and 2. In contrast to the classical closed basin approach, which requires the WBC transport to be equal and opposite to the interior Sverdrup transport so that there is no net meridional transport (i.e., $T = 0$), we do not require the two transports to have any particular relationship. This implies that there can be a net meridional transport. For reasons that will become momentarily apparent, (2.10a,b) are now rewritten in the form,

$$f_1 T = \frac{g'}{2}(h_{\mathbf{C}}^2 - h_{\mathbf{D}}^2) - \int_{\mathbf{D}}^{\mathbf{C}} \frac{\tau^x}{\rho}\, dx \tag{2.11a}$$

$$f_2 T = \frac{g'}{2}(h_{\mathbf{B}}^2 - h_{\mathbf{A}}^2) - \int_{\mathbf{A}}^{\mathbf{B}} \frac{\tau^x}{\rho}\, dx. \tag{2.11b}$$

By subtracting (2.11b) from (2.11a) and taking into account the eastern boundary condition (2.8) and the separation condition (2.9) we find the surprisingly simple relationship,

$$T = \frac{1}{f_1 - f_2}\left[\int_{\mathbf{A}}^{\mathbf{B}} \frac{\tau^x}{\rho}\, dx + \int_{\mathbf{B}}^{\mathbf{C}} \frac{\tau^x \sin\alpha}{\rho}\, ds + \int_{\mathbf{C}}^{\mathbf{D}} \frac{\tau^x}{\rho}\, dx\right], \tag{2.12}$$

which is our desired formula. It should now be clear why we start and finish our integration at the separation points; only these two locations correspond to zero pressure along the western boundary. Relation (2.12) gives the combined (wind and high-latitude cooling) transport in terms of the wind field and the separation latitudes *alone*. The main difference between (2.12) and the analogous formula derived by Nof (1998) for the Pacific is that his formula does not involve f_1. This is due to the fact that the Indonesian Throughflow is situated south of the Kuroshio's separation latitude.

To understand what (2.12) means we shall consider a few examples. First, we shall consider the simplest possible case where there is no asymmetry in either the wind field or the continents, that is, the only asymmetry is in the high-latitude cooling which enters the problem through the (given) WBC separation latitudes. In this special case the second term in (2.12) drops out. To illustrate the properties of this case, we chose an ocean 6000 km broad driven by the globally averaged Hellerman and Rosenstein (1983) winds [see Nof's (1998) Fig. 4a for a plot of the average wind versus latitude]. Figure 4 shows the results for two hypothetical cases; one corresponds to a net meridional transport of 12 Sv (upper panel), and the other to a net transport of 4 Sv (lower panel).

For the second example we add an asymmetry in the wind field but retain the symmetrical geometry. Namely, the eastern boundary is still meridional so that there is no asymmetry in the shape of the continents. For this special case the second term still drops out and there is no meridional transport (i.e., $T \equiv 0$) unless there is some *asymmetry* in either the wind field or the position of the separation latitude (controlled by the cooling). For instance, consider a hypothetical rectangular ocean 5000 km broad with boundary currents detaching from the western boundary at 40°N and 40°S. There is no wind stress along 40°N and an eastward wind corresponding to a stress of 2 dyn cm^{-2} is blowing along 40°S. According to (2.12), such an ocean will have a northward interhemispheric transport of 5 Sv. Recall that the associated cooling enters this example through our choice of the 40°N and 40°S separation latitudes. Without cooling, such separation latitudes cannot be maintained and the separation points would drift to new latitudes that [according to (2.12)] give no meridional transport.

For the third example we now add an asymmetry in the geography. In this case the wind along the southern section (**AB**) is acting over a different distance than the wind along the northern section (**DC**) so that even identical winds cause a meridional transport [provided that the wind stress along the eastern boundary (**BC**) is not identical to those winds]. For instance, consider now a trapezoidal ocean extending 5000 km along 40°N and 10 000 km along 40°S with currents separating again at 40°N and 40°S. As in the second example, the ocean is subject to no zonal wind stress along the northern boundary and an eastward wind corresponding to 2 dyn cm^{-2} along the southern boundary. We also specify here a linear wind stress dependence along the eastern boundary. According to (2.12), such an ocean will have a net northward transport of 8 Sv, which is 60% greater than the net transport in the rectangular ocean. All three examples illustrate that only severe interhemispheric asymmetries generate significant interhemispheric

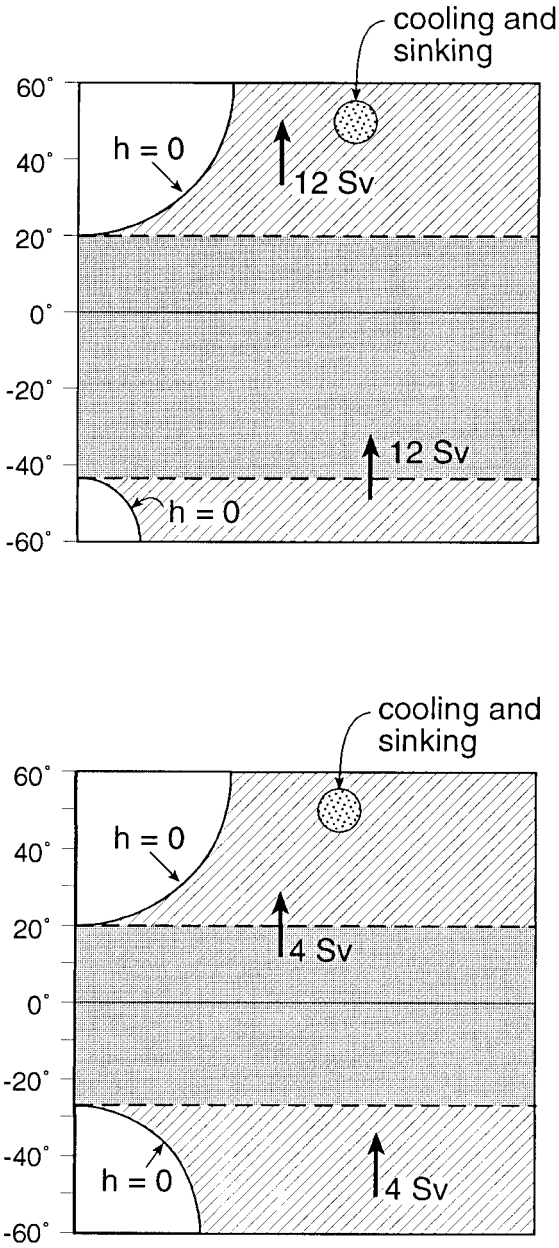

FIG. 4. Two situations corresponding to high-latitude cooling and wind, which force 12 Sv (upper panel) and 4 Sv (lower panel) across the equator. Shaded areas denote the fluid obeying our formula. Hatched areas are regions where diabatic cooling is allowed. Dotted regions are areas where sinking takes place.

flows; mild asymmetries generate very weak meridional flow.

3. Properties of the transport

As mentioned, the expression for the meridional transport (2.12) does not contain any cooling explicitly because cooling enters the problem only through the position of the separation points, which must adjust to the amount of imposed overturning. In other words, a change in the cooling would force the WBC separations to migrate southward or northward until they find the latitude where the wind stress can accommodate the new imposed cooling and (2.12) is again satisfied.

For example, a state of no-meridional transport and a no-overturning state (corresponding to the symmetrical winds discussed earlier and symmetrical separation latitude) can change to a state with a net northward transport of 12 Sv (in a rectangular ocean 6000 km broad) if, due to high-latitude cooling, the northern separation latitude moves to 20°N and the southern separation latitude moves to 43°S. Similarly, time-dependent variations in the wind stress would also cause a shift in the position of the separation points. Clearly, changing the wind stress in the South Atlantic is not going to change the overturning rate but, rather, it will force one or both gyres to migrate meridionally until new separation latitudes that fit the new wind stress pattern [according to (2.12)] are found. Also, note that, according to (2.12), in the absence of wind there can be no meridional flow even if there is asymmetrical high-latitude cooling. This (apparent) unphysical situation results from the simple fact that with high-latitude cooling alone there would not be any separation of WBC south of the cooling region so that (2.12) does not apply.

It is important to realize that, in this model, the separation of the WBC does not necessarily occur along the latitude of vanishing wind stress curl. Instead, it occurs where the thermocline depth along the wall vanishes, that is, in the Charney (1955) manner where, due to the increase of the Coriolis parameter with y, a poleward flowing WBC ultimately reaches a point where the thermocline surfaces along the coast. Charney's separation includes inertial nonlinear terms, which are absent from this model, but the essence of the separation is identical in the two cases. Alternatively, one can think of our separation as Parsons' (1969) separation without the condition of no net meridional flow across the ocean.

To see this more clearly, recall that the idea of WBC separation occurring at the latitude of vanishing wind stress curl originates in the assumption of a boundary current transport being equal and opposite to the interior Sverdrup transport. The theory is that, in this scenario, when the interior transport vanishes (due to zero wind stress curl), then the WBC meridional transport must vanish as well, implying a separation. In our case, however, the WBC transport is not necessarily equal and opposite to the interior transport because *there is a net* meridional transport. This implies that the separation does not occur at the zero wind stress curl latitude unless it so happens that the net meridional transport is zero.

Following Nof (1998), it is a simple matter to extend the results of the simple reduced-gravity model with one active layer to a continuously stratified upper ocean overlying again a stagnant intermediate layer. Using the Boussinesq approximation and the vertically integrated equations in spherical coordinates, one ultimately arrives at the formula,

$$T = \int_{\mathbf{ABCDEF}}^{\tau'} dl \Big/ \rho(f_1 - f_2), \tag{3.1}$$

where T is the total transport and, as before, the integration is done in a horseshoe manner in the sense that it is not an integration over a closed path but rather an integration over an open path that does not contain section **FA**. Note that (3.1) contains both zonal and meridional winds and that upwelling due to Ekman flows is a part of our vertically integrated transport.

As in the single-moving-layer case, (3.1) contains both wind-driven motions and diabatic motions imposed by high-latitude cooling (poleward of the separation latitude). This cooling does not enter (3.1) explicitly but does enter it implicitly through the separation latitude and the associated integration paths **ABCDEF**.

4. Numerical simulations

To examine the validity of the formula (2.12) we consider now an application of a reduced gravity MICOM (Miami Isopycnal Coordinates Ocean Model) to a rectangular basin spanning both hemispheres. To represent the cooling we specify a (mass flux) source in the southeast corner (south of the Brazil Current separation latitude) and a sink in the northeast corner (north of the Gulf Stream separation). We shall vary the transport, measure the location of both WBC separations, and then plot the computed separation formula transport versus the specified transport.

The numerical model

We use a reduced gravity version of the MICOM developed by Bleck and Boudra (1981, 1986), and later improved by Bleck and Smith (1990). The advantage of this model is the use of the ''flux corrected transport'' algorithm (Boris and Book 1973; Zalesak 1979) for the solution of the continuity equation. This algorithm employs a higher order correction to the depth calculations and allows the layers to outcrop and stay positive definite. The resulting scheme is virtually nondiffusive and conserves mass. For these reasons, the model is the most suitable model for our problem. The active layer is an enclosed feature, while the rest of the layer has zero depth.

The modeled basin is a rectangle extending from 60°S to 60°N. The interhemispheric exchange is established by withdrawing water from the northeast corner of the basin and forcing an equal amount back into the basin along the southeast corner.

The equations of motion are the two momentum equations,

$$\frac{\partial u}{\partial t} + u\frac{\partial u}{\partial x} + v\frac{\partial u}{\partial y} - (f_0 + \beta y)v = -g'\frac{\partial h}{\partial x} + \frac{\nu}{h}\nabla \cdot (h\nabla u) + \frac{\tau_x}{\rho h} - ku \quad (4.1)$$

$$\frac{\partial v}{\partial t} + u\frac{\partial v}{\partial x} + v\frac{\partial v}{\partial y} + (f_0 + \beta y)u = -g'\frac{\partial h}{\partial y} + \frac{\nu}{h}\nabla \cdot (h\nabla v) + \frac{\tau_v}{\rho h} - kv, \quad (4.2)$$

and the continuity equation,

$$\frac{\partial h}{\partial t} + \frac{\partial (hu)}{\partial x} + \frac{\partial (hv)}{\partial y} = 0, \quad (4.3)$$

where the notation is conventional.

The model uses the Arakawa (1966) C-grid. The u-velocity points are shifted one-half grid step to the left from the h points, the v-velocity points are shifted one-half grid step down from the h points, and the vorticity points are shifted one-half grid step down from the u-velocity points. This grid allows for reducing the order of the errors in the numerical scheme. The grid scale is 15 km, and the solution is advanced in time using the leapfrog scheme with a time step of 540 s. The velocity fields are smoothed in time in order to stabilize the numerical procedure. The velocities for the weightless grid points are set to zero.

To make our runs more economical, we artificially magnified both β and the wind stress (by a factor of 5 and 10, respectively) and artificially reduced both the meridional and zonal basin scales (again by a factor of 5 and 10, respectively). With these changes, our β was 10×10^{-11} m^{-1} s^{-1}, the zonal basin size was 600 km, the meridional basin size was 1320 km (in each hemisphere), and the Coriolis parameter remained unaltered (for the new latitudes). The linear drag coefficient, k, was also increased by a factor of 10 (to 1×10^{-6} s^{-1}) so that the increased wind stress is balanced. With a grid size of 15 km, an (unaltered) reduced gravity of 1.5×10^{-2} m s^{-2} and an undisturbed depth of 300 m, our runs lasted for about 40 minutes (each) instead of a week or so that each run would have lasted had we not modified β, the wind stress, and the basin size.

The downside of the above modifications is an unnaturally large ratio between the eddy size (the Rossby radius) and the basin size. As we shall shortly see, this is not really a difficulty in our runs because in our case the eddies do not play a major role in the meridional mass exchange. Furthermore, this unnatural eddy:basin ratio issue can be easily resolved by using a very large horizontal eddy viscosity coefficient (16 000 m^2 s^{-1}) that eliminates any long-lived eddies such as Gulf Stream rings. This essentially implies that our model is not an eddy-resolving model. For completeness we also ran a series of numerical simulations with a much smaller eddy viscosity (ν = 1000 m^2 s^{-1}). The implications of these numerical values for the frictional coefficient are discussed below.

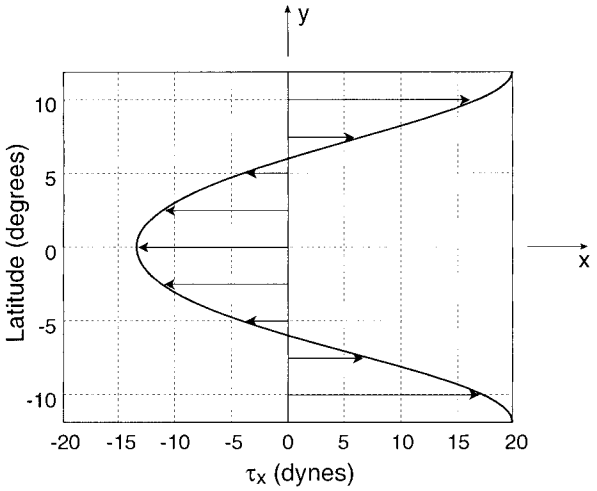

FIG. 5. The magnified (and simplified) zonal wind stress as a function of the adjusted meridional scale (used in the numerical simulations).

The simplified wind stress profile that we used is shown in Fig. 5 and a typical (symmetrical) depth and transport structure without any cross-equatorial flow is shown in Fig. 6a. With a forced cross-equatorial flow the fields become asymmetrical as shown in Fig. 6b. Figure 6b also shows how the current (shaded) crosses the equator. It begins along the eastern boundary of the South Atlantic and proceeds westward as a south equatorial current. As earlier studies predicted (see, e.g., Killworth 1991) it then crosses the equator as a WBC. It finally reaches the northeast corner after progressing along the northern edge of the gyre.

Figure 7 shows the observed (numerical) adjustments and movements of the WBC separations in response to the cross-equatorial flow and Fig. 8 displays a comparison of the analytical solution to the numerical simulations. Figure 8 shows that, even with the large eddy viscosity (16 000 m^2 s^{-1}), there is an exceptionally good agreement between the nonlinear numerical simulations and the quasi-linear analytical computation. This remarkable agreement shows that full nonlinearity (included in the numerics but absent from the analytics) is unimportant. Also, the small difference between the two lines (corresponding to the two different viscosities) in Figs. 7 and 8 shows that the position of the WBC separation points is not very sensitive to the horizontal frictional coefficient. This is because, as just mentioned,

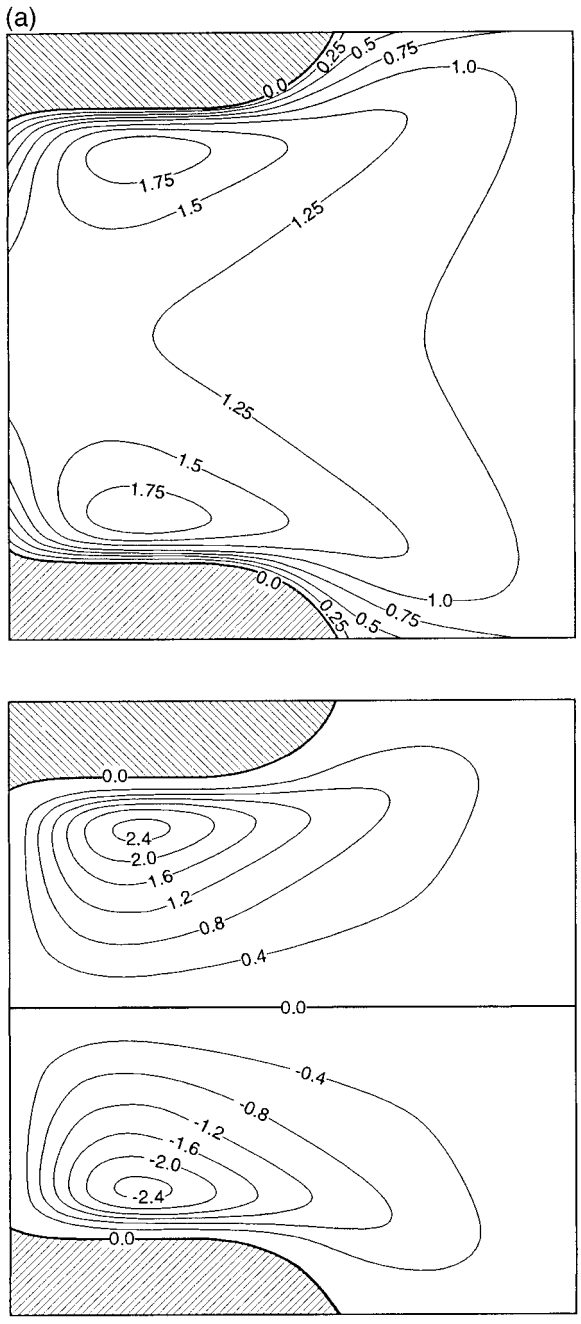

FIG. 6a. Nondimensional thickness contours (upper panel) and transport contours (lower panel) for the case of no net meridional transport and high viscosity ($\nu = 16\,000$ m^2 s^{-1}). As expected, both patterns are symmetric relative to the equator. The thickness is nondimensionalized with the undisturbed depth ($H = 300$ m) and the transport by $g H^2/2f_0$ (where $g = 2 \times 10^{-2}$ m s^{-2}, $H = 300$ m, and $f_0 = 0.9 \times 10^{-4}$ s^{-1}). Hatched regions denote regions where there is no upper layer.

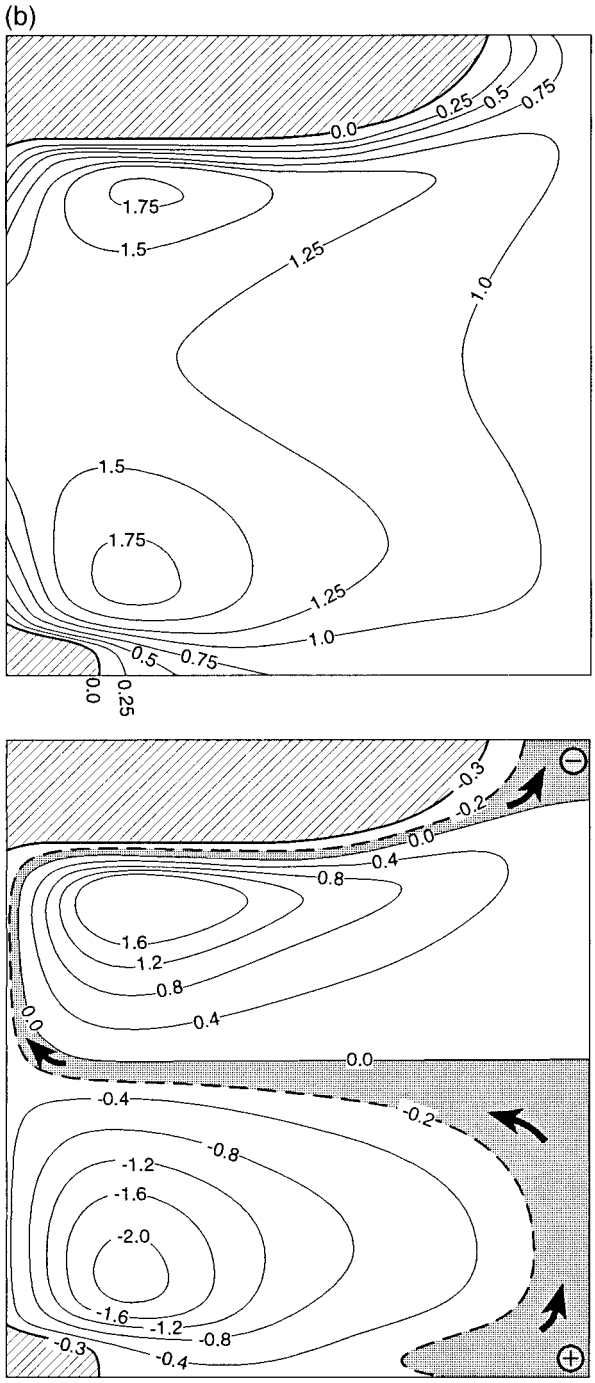

FIG. 6b. The same as Fig. 6a but with a net (nondimensional) meridional transport of approximately 0.3. The transport is forced by a specified source (+) in the southeast corner and a sink (−) in the northeast corner. The core of the net cross-equatorial flow is shaded. Hatched regions denote that there is no upper layer. Note that the separation latitude of the simulated **BC** moved considerably toward the south so that the fields are no longer symmetrical. Also, note that the cross-equatorial flow follows an ''S-shaped'' pattern; it begins in the Southern Hemisphere as a flow along the eastern boundary. It then proceeds as a south equatorial current and crosses the equator as a WBC. It finally reaches the northeast corner via the northern part of the gyre. It is later argued that, although such an exchange is dynamically possible, the observed positions of the WBC separations do not possess the asymmetry required for such an exchange.

mesoscale eddies do not play a crucial role in our interhemispheric mass transport.

Note that even our ''moderate'' eddy viscosity coefficient ($\nu = 1000$ m^2 s^{-1}) is still larger than what may

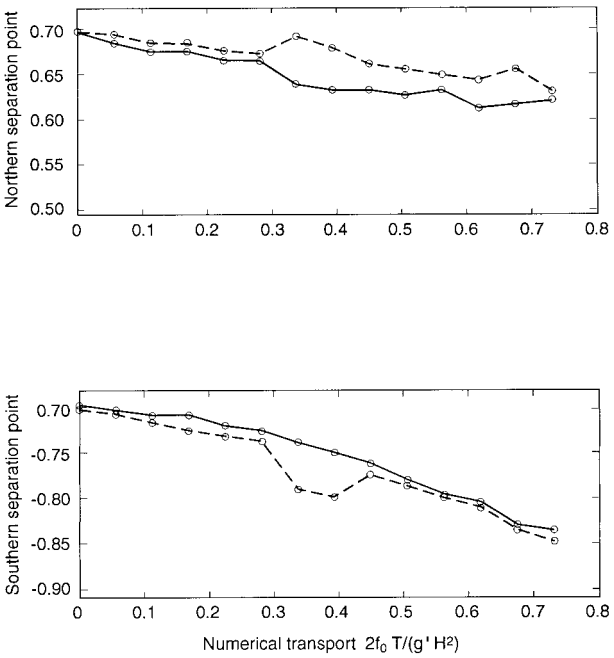

FIG. 7. The position of the northern WBC separation (upper panel) and southern WBC separation (lower panel) for two series of numerical simulations with a forced cross-equatorial flow. All are nondimensionalized with the basin's meridional scale (1320 km). The solid line corresponds to high viscosity simulations (with $\nu = 16\,000$ $m^2\ s^{-1}$), whereas the dashed line corresponds to average viscosity ($\nu = 1000\ m^2\ s^{-1}$). Note that the migration of the southern WBC separation latitude is more pronounced than that of the northern WBC separation.

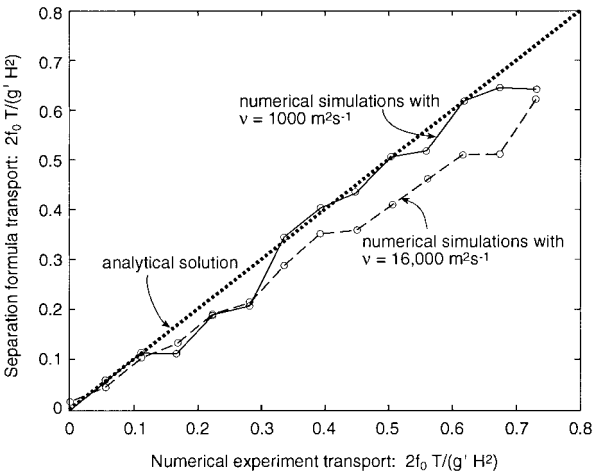

FIG. 8. A comparison of the analytical solution (thick dotted line) to the two series of numerical experiments. The high viscosity experiment ($\nu = 16\,000$ $m^2\ s^{-1}$) is shown with the dashed line and the moderate viscosity simulations ($\nu = 1000\ m^2\ s^{-1}$) with the solid line. Note that the agreement is excellent despite that the analytical solution is based on quasi-linear equations whereas the numerical model is based on the primitive equations. The error in the numerics and the associated graphics is represented by the thickness of the lines. The excellent agreement suggests that fully nonlinear processes (neglected in the analytical comptations but included in the numerics) are not very important.

be considered an ''average eddy viscosity'' for general circulation isopycnic models. (For an ''average diffusion speed'' of 1 cm s^{-1} and a grid size of 15 km it is 150 $m^2\ s^{-1}$.) However, we could not lower it any further due to numerical instability. We see (from Fig. 8) that almost all simulations are below the analytical prediction and that the high viscosity experiments are further away from the analytical solution than the moderate viscosity experiments. This larger discrepancy between the two models occurs because higher viscosity forces the gyre to ''flatten out'' so that the separation latitudes are pushed poleward toward regions with higher wind stress.

5. The interhemispheric transport in the Atlantic

We used COAD annual mean winds (Woodruff et al. 1987) with a drag coefficient of 1.6×10^{-3} [which is the appropriate coefficient for winds (such as ours) with a speed of less than 6.7 m s^{-1} (see, e.g., Hellerman and Rosenstein (1983)]. We identified the separation points to be the annual mean intersection of the observed $\sigma_\theta = 26.8$ isopycnal [taken from the Levitus (1982) climatology] with the coast at a depth of 100 m. This turns out to be roughly 36°N (see Fig. 3) but the exact latitude does not really matter since it is the wind stress rather than the wind stress curl that enters our calculations. Namely, the wind stress is much less sensitive than the wind stress curl to variations in latitude so that the result is not very sensitive to the choice of $\sigma_\theta = 26.8$. We chose the 26.8 σ_θ because it corresponds to the maximum density gradients so that it effectively represents the thermocline. The choice of a 100-m depth for the isopycnal intersection with the coast was made in order to avoid mixed layer effects and is very reasonable. Since the speeds within the western boundary currents are high [$\sim O(1$ m $s^{-1})$], the intersection of the 26.8 σ_θ isopycnal with the free surface of an ocean without a mixed layer would be no more than a distance of $O(10$ km) away from our chosen location at a depth of 100 m.

Also, by looking at the *annual mean position* of the 26.8 σ_θ intersection, the seasonal migration of the Brazil–Malvinas confluence (see, e.g., Matano 1993; Lebedev and Nof 1996) is filtered out. Note that, since the Malvinas Current is not a part of our model, it is also implicitly assumed here that, in an ocean without a Malvinas Current, the separation of the Brazil Current would occur at a location that is not very far from the presently observed separation. This assumption is justified because our calculations involve the wind stress and not the wind stress curl. The wind stress is not very insensitive to variations in latitude and even a Malvinas-induced variation of as much as a few hundred kilometers would not significantly affect our results.

Along the horseshoe path (Fig. 3) the integration was done over $2° \times 2°$ boxes. With the aid of (3.1) one finds that the first leg (section **AC**, Fig. 3) contributes 2.055

Sv, the second leg (section **DC**) 0.0845 Sv, and the third leg (section **DF**) contributes 1.533 Sv. This leads to a surprising result—a negligible net meridional transport of less than 1 Sv. It implies that, with our (no low and midlatitude upwelling) model, there is virtually no net meridional flow into the North Atlantic of water lighter than 26.8 σ_θ. In other words, according to our model, the concept of a conveyor consisting of pure surface Atlantic water flowing northward due to a combined effect of high-latitude cooling and wind is in question. We shall address this issue in detail in following subsections. Before doing so, however, it is appropriate to discuss the role that Agulhas rings play in the problem.

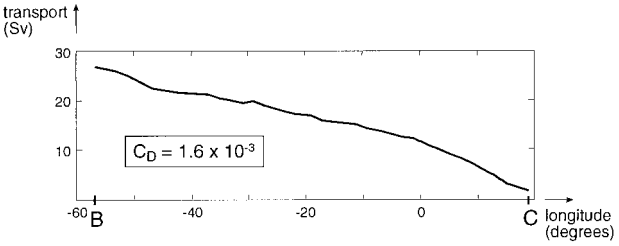

FIG. 9. The integrated Sverdrup transport as a function of longitude (to the west of the Cape of Good Hope) along cross section **ABC** (shown in Fig. 3). The total amount of northward flowing water in the interior is 28 Sv. It is argued that all of this warm water is ultimately expelled from the South Atlantic via the Brazil Current and its extension.

a. Agulhas rings

Both observations and wind-driven circulation models show transfer of Indian Ocean thermocline water into the South Atlantic (Boudra and Chassignet 1988; Semtner and Chervin 1988; Gordon and Haxby 1990). Most of the leakage is achieved via Agulhas rings (Olson and Evans 1986; Lutjeharms and Gordon 1987; Lutjeharms and Van Ballegooyen 1988), but additional Indian Ocean waters are injected into the Atlantic via plumes (Olson and Evans 1986; Lutjeharms 1988; Lutjeharms and Valentine 1988). Also, surface waters are sometimes entrained by the Benguela Current (Nelson and Hutchings 1983; Shannon 1985). Estimates of the above leakage vary considerably due to various measuring techniques and (perhaps) due to actual variability.

Gordon et al. (1987) arrived at an estimate of 10 Sv for water entering the Atlantic in 1983 whereas Whitworth and Nowlin (1987) observed a much larger transport of 20 Sv in 1984. Bennett (1988), on the other hand, arrived at lower values of 6.3 and 9.6 Sv for 1983 and 1984. From these amounts that enter the Atlantic, Bennett argues that only 2.8 Sv are warm Indian Ocean water. Stramma and Peterson (1990) find an Indian to Atlantic transfer of 8 Sv whereas Gordon and Haxby's (1990) inventory of rings suggest a transport of 10–15 Sv. McCartney and Woodgate-Jones' (1991) definition of an eddy corresponds to a smaller feature than that considered by Gordon and Haxby (1990) and, consequently, they arrive at a smaller estimate of 2–5 Sv. Byrne et al. (1995) estimated the flux to be at least 5 Sv; the most recent and most extensive estimate is that of Goñi et al. (1997), who arrive at an average influx of no more than 4–5 Sv. Since it is the most updated estimate, we shall use this latter value as a typical mass flux of warm Indian Ocean water into the South Atlantic [even though it is somewhat smaller than previous values (see also van Ballegooyen et al. 1994; Duncombe Rae et al. 1996)].

Olson and Evans (1986) estimate that the rings translate toward the northwest at a rate of 5–8 cm s^{-1}. Goñi et al. (1997) arrive at a similar rate of 5–14 cm s^{-1}. A fourth of this speed is probably due to the familiar β-induced speed, which for rings with a diameter of 400–500 km, a depth of 800 m, and a reduced gravity of 2×10^{-2} m s^{-2} is no more than 1.5 cm s^{-1}. [This can be easily verified by recalling that such rings translate at a speed that is smaller than 0.4 βR_d^2, where R_d is the Rossby radius based on the ring's maximum depth (see, e.g., Nof 1981)]. Another fourth of the observed migration speed is due to advection by the local Sverdrup flow (see Fig. 6) and the remaining half (3–7 cm s^{-1}) cannot be clearly accounted for. [It can possibly be due to bottom topography that increases the migration rate (see, e.g., Dewar and Gailliard 1994 but also Kamenkovich et al. 1996 where a counterexample of a reduced rate is given) or due to a dipolar structure (Radko 1997).] Regardless of the causes for this unaccounted speed, we can conclude that out of the 4–5 Sv influx, about 1.5 Sv is due to advection by the surrounding flow that obeys Sverdrup dynamics and, hence, is *included* in both the formula and the numerics. Namely, in our calculations, 3–4 Sv, at the most, are neglected because of the absence of the rings' self-propulsion mechanism. This is a relatively small amount compared to the observed 10 Sv of interhemispheric flow.

Computation of the meridional Sverdrup transport shows that along cross-section **BC** (shown in Fig. 3) the flow is northward and amounts to a total of about 28 Sv (Fig. 9). According to our model these 28 Sv must exit the basin to the south via the Brazil Current and its extension.

b. Implications of our results

Since a considerable amount of water does sink in the North Atlantic and flows southward as NADW, some process that is not included in our nondiffusive (i.e., no upwelling) thermocline model must take place. All traditional wind-driven upper-layer dynamics as well as surface cooling in high latitudes are included in the model, suggesting that our inactive intermediate water (i.e., water with a potential density greater than 26.8) must play an important role. In our model this resting intermediate water is situated poleward of the curves along which the $\sigma_\theta = 26.8$ surface strikes the free surface and under the upper layer ($\sigma_\theta < 26.8$) throughout

the Atlantic. We shall shortly show that, if the conveyor water is indeed moving northward as the observations suggest, then the intermediate water must somehow upwell into the upper layer within the limits of the Atlantic Ocean. This is consistent with Matano and Philander (1993), who suggested that upwelling should occur in the South Atlantic.

Upwelling à la Goldsbrough (1933) can be easily added to our two-layer model (described earlier in section 2). Goldsbrough's approach (originally used to describe evaporation and precipitation) is to add a source or a sink only in the continuity equation leaving the momentum equations unaltered. Even though the sink or source may correspond to water with a density different than that of the upper layer, the Goldsbrough approach is to ignore this difference to first order. In this context it is appropriate to point out that, in a way, our upwelling represents cooling because it brings colder water to the upper layer (see, e.g., Veronis 1976).

As in Nof (1998), with the Goldsbrough approach the only alteration to our Eqs. (2.1)–(2.3) is that, instead of (2.3), we now have,

$$U_x + V_y - w = 0, \tag{5.1}$$

where w is the specified upwelling at the base of the thermocline. Equations (2.1) and (2.2) remain unaltered, but the Sverdrup transport now takes the modified form,

$$\beta V = -\frac{1}{\rho}\frac{\partial \tau^x}{\partial y} - fw. \tag{5.2}$$

The modified form of (2.11a,b) is

$$f_1(T + Q_u) = \frac{g'}{2}(h_{\mathbf{C}}^2 - h_{\mathbf{D}}^2) - \int_{\mathbf{D}}^{\mathbf{C}} \frac{\tau_x}{\rho}\, dx \tag{5.3a}$$

$$f_2 T = \frac{g'}{2}(h_{\mathbf{B}}^2 - h_{\mathbf{A}}^2) - \int_{\mathbf{A}}^{\mathbf{B}} \frac{\tau_x}{\rho}\, dx, \tag{5.3b}$$

where Q_u ($=\iint w\, dx\, dy$) is the total upwelling taking place within the confinement of the integration area, and, as before, T is the transport entering the Atlantic from the south. By subtracting (5.3b) from (5.3a) and, again, taking into account the eastern boundary condition (2.8) and the separation condition (2.9), we find

$$f_1 Q_u + (f_1 - f_2)T = \int_{\mathbf{A}}^{\mathbf{B}} \frac{\tau_x}{\rho}\, dx + \int_{\mathbf{B}}^{\mathbf{C}} \frac{\tau_x \sin\alpha}{\rho}\, dx + \int_{\mathbf{C}}^{\mathbf{D}} \frac{\tau_x}{\rho}\, dx = \int_{\mathbf{ABCD}} \frac{\tau^l\, dl}{\rho}, \tag{5.4}$$

where **A**, **B**, **C**, and **D** correspond to the integration path shown in Fig. 1. Clearly, relation (5.4) is also valid in spherical coordinates. However, in this upwelling case, it does not make any sense to speak about a stratified upper layer because it is hard to imagine how upwelled water can immediately accept the surrounding stratified density as it is injected into the fluid. Consequently, we consider here an upper layer with uniform density, an outcropping interface, and a stagnant intermediate layer. Note that (5.4) is quite different from Nof's application of the separation formula to the Pacific, which does not involve f_1. Also note that it certainly would have been better to add a reliable mixing parameterization to our upwelling scenario but this is left as a subject for future investigation.

In our scenario, the application of the right-hand side of (5.4) to the Atlantic is the same as before, that is, it corresponds to a transport of less than one Sverdrup. Furthermore, since $f_1 \approx -f_2$ we find that $T \approx -Q_u/2$. This means that the total upwelled water Q_u must split into roughly two equal parts. One part flows northward (past the separation latitude) and ultimately sinks in the North Atlantic. The other half must flow southward and exit the South Atlantic via the Brazil Current (Figs. 10a,b). This somewhat odd result implies that the amount of water upwelled into the thermocline throughout the low and midlatitude Atlantic must be twice as much as the net amount transported northward.

How the upwelling of 20 Sv is achieved within the limits of the Atlantic Ocean is not entirely obvious. Recent measurements of diapycnal diffusivities (Ledwell et al. 1993; Toole et al. 1994; Kunze and Sanford 1996) suggest an interior mixing coefficient of no more than 0.1 $\text{cm}^2\ \text{s}^{-1}$. For an area of 10 000 km $\times$ 5000 km and a mean thermocline depth of 500 m, such a diffusivity coefficient would lead to an upwelling of merely 1 Sv. However, these slow mixing coefficients are not in agreement with budget calculations, which suggest much higher coefficients in regions where there are intense currents. For example, Qiao and Weisberg (1997) suggest mixing coefficients that would allow 20 Sv to be *easily upwelled* into the thermocline over the equatorial region alone. Similarly, more than a decade ago, Roemmich (1983) suggested that 6 Sv are converted to thermocline water somewhere between 8°S and 8°N. Both of these studies suggest that most of the mixing probably occurs in special locations and not in the ocean interior. This is supported by Lueck and Mudge (1997), who, on the basis of measurements of energy dissipation, suggest that shallow seamounts induce mixing that can be 100 to 10 000 times larger than the mixing away from the seamount. Bottom topography also produces very strong mixing (Polzin et al. 1996, 1997). As with many other calculations, our model requires a vertical diffusivity coefficient that, on average, is an order of magnitude higher than that observed in the interior of the ocean. It is quite possible that, as others have suggested, intense mixing and entrainment take place along the boundaries of the ocean, along the equator, and in the vicinity of seamounts.

An alternative to the Atlantic upwelling scenario is that the model is flawed or that Goñi's et al. (1997) estimates of Agulhas rings transfer are grossly below the actual values. (Recall that the rings are partially

included in both our linear interior dynamics analytical model and in our noneddy-resolving primitive equation numerical model.) Four aspects of the model could perhaps be problematic. The first is the Gulf of Guinea where the boundary of the continent is approximately zonal so that a strong boundary current (not captured by our eastern boundary condition) can perhaps develop. Examination of the offshore Sverdrup transports (which can produce the boundary current in question) as well as Hisard's et al. (1986) measurements (conducted during 1984, an admittedly anomalous year) reveal, however, that an average 10 Sv transport in the Gulf of Guinea is highly unlikely. This possibility is, therefore, rejected. The second possibility is that eddy-driven flows in the southeastern Atlantic (neglected in both the analytics and numerics) transfer the excess amount of water necessary for the closure. Recent measurements of the Benguela Current (Peterson and Stramma 1991; Clement and Gordon 1995; Garzoli et al. 1996; Garzoli et al. 1997) suggest, however, that there is a difference of merely a few Sverdrups between the calculated Sverdrup transport (included in both the analytical and the numerical models) and the measured Benguela Current transport. This amount is not sufficient to explain the required 10 Sv and, therefore, the second possibility is also rejected.

The third possibility is that the intermediate layer is somehow directly responsible for the meridional upper-water transfer, that is, that the neglected pressure gradients in the intermediate layer are responsible for forcing 10 Sv of upper thermocline water northward. Using scaling arguments, it is easy to demonstrate that, in order for this to happen, the northward speeds in the intermediate layer must be of the same order as the northward upper-water velocity. Since, on average, the intermediate layer is 8–10 times thicker than the upper layer, this implies a, highly unlikely, northward transport of 80–100 Sv in the intermediate layer. In view of this, the third possibility is also rejected.

The fourth possibility is that the model requires a choice of a lighter σ_θ surface (i.e., a ligher upper layer) of, say, 26.0 σ_θ instead of our choice of 26.8 σ_θ. This would make the required upwelling consistent with the more traditional approach [see, e.g., Roemmich (1983) and Fig. 9 in Speer et al. (1996)]. Although a somewhat lighter σ_θ surface than 26.8 can perhaps be chosen, the surface 26.0 σ_θ is much too light for two reasons. First, it is much lighter than the density corresponding to the maximum density gradient and, second, it intersects the eastern boundary south of the model domain (see point **C**, Fig. 2 or point **D**, Fig. 3) making the application impossible. The reader is also reminded at this point that, since the model uses the wind stress rather than the curl of the wind stress as input, it is very insensitive to the choice of the separation latitude as long as it is within a reasonable range.

It should be pointed out here that other effects such as JEBAR and bottom torque (Myers et al. 1996), corners and local geography (Dengg 1993; Ou and DeRuijter 1986), and lateral inflows (Ezer and Mellor 1992; Thompson and Schmitz 1989) are also excluded from our model. Although these processes affect the position of the separation, their effect is limited to several degrees. As mentioned earlier, our formula is very insensitive to the position of the separation (because it involves the wind stress rather than the curl of the wind stress) so that these issues have no impact on our results.

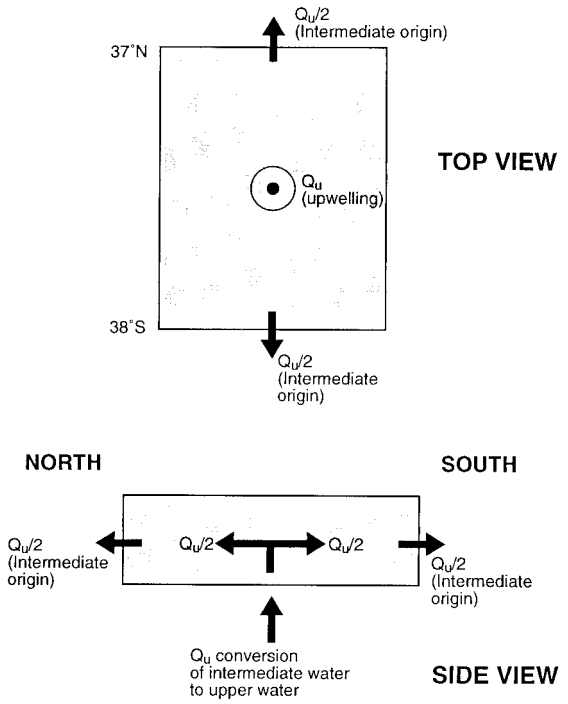

FIG. 10a. The suggested circulation pattern of thermocline water in the Atlantic. Our formula shows that, without low and midlatitude upwelling in the Atlantic, virtually no upper water can be forced northward (save perhaps the neglected self-induced transport of Agulhas rings and other eddy-driven flows) across the Atlantic equator. Furthermore, it illustrates that any conversion of intermediate water to upper water must be equally split between a northward and a southward current, that is, if, say, Q_u is upwelled throughout the Atlantic, then $Q_u/2$ must be flowing northward and $Q_u/2$ must be flowing southward (see Fig. 10b).

Finally, a comment should be made regarding the relationship between our study, which shows a net surface water flow of about 10 Sv southward, and Saunders and King's (1996) inverse analysis, which shows a net surface flow of 10 Sv northward. At this stage, we do not know how the two contradictory conclusions can be reconciled. We can only say that the two studies are very different and may involve, at least some, different water masses (e.g., bottom water is included in Saunders and King's analysis but neglected in ours). Another possibility is that the storage of warm water in the Atlantic is subject to oscillations [occurring on a frequency of O(100 yr) or less] superimposed on our average circulation pattern. Such oscillations would correspond to the Atlantic upper layer draining and filling up alter-

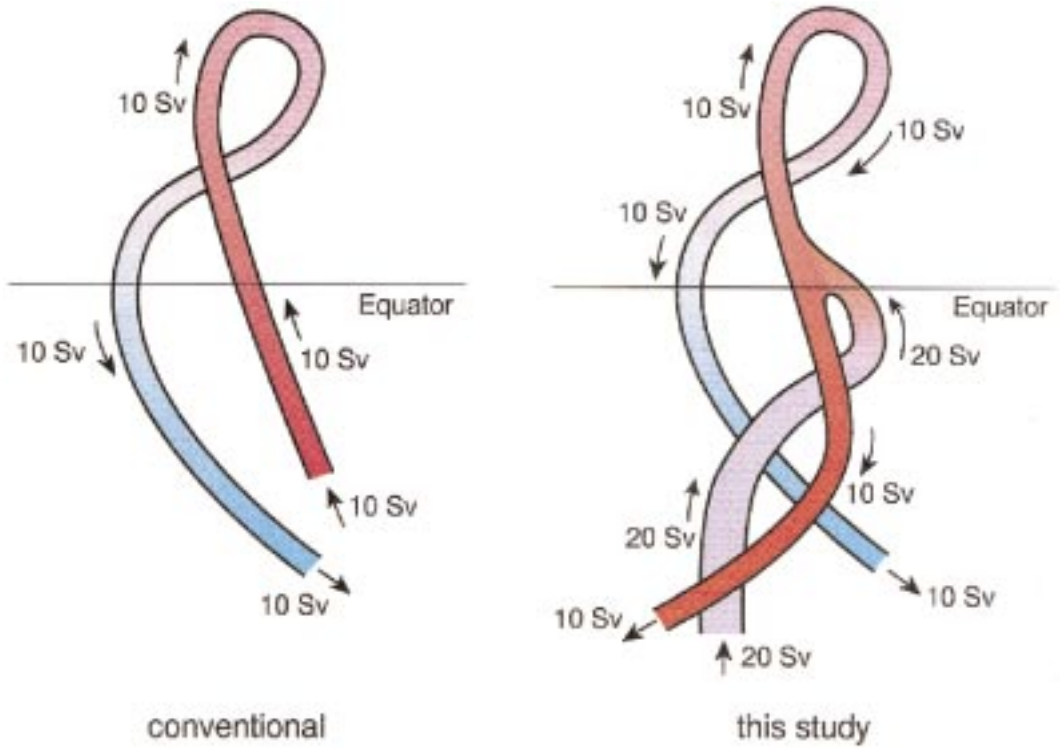

FIG. 10b. The conventional view of the conveyor's upper limbs in the Atlantic (left panel) and the very different structure proposed by our study (right panel). In contrast to the common view that most of the upwelling occurs in the Indian and Pacific Oceans (rather than the Atlantic), our model suggests that the upwelling occurs within the limits of the Atlantic. Namely, the model suggests that without upwelling (in the Atlantic) no water at all can sink in the North Atlantic. Furthermore, our model shows that only half of the total upwelled water sinks in the North Atlantic. The remaining other half must exit the South Atlantic (via the Brazil Current).

nately. This would add an $O(10)$ Sv fluctuation to the net transport in and out of the Atlantic, and it is quite possible that Saunders and King's measurements were done during a filling up stage.

6. Summary and discussion

To circumvent solving the (incredibly complicated) wind–thermohaline problem we have adopted a new technique where the observed positions of western boundary current (WBC) separation are blended into an analytical model. These positions are unique in that they provide useful information about the pressure fields. We have considered a model where the low and midlatitude interior is governed by Sverdrup dynamics and the WBC are dissipative in nature. Surface cooling and sinking are limited to latitudes higher than the separation latitudes and enter the problem through the WBC separation latitude. This analytical model includes some nonlinearity (through the pressure terms) but the inertial terms are neglected and the Coriolis terms dominate the motions.

The model is applied to a basin extending from the tip of South Africa in the Southern Hemisphere to Cape Hatteras where the Gulf Stream separates in the Northern Hemisphere. It is open on the southern side so that a free exchange with other oceans is allowed. A net northward interhemispheric flow of upper water is permitted, that is, the WBC transport is not necessarily equal and opposite to the integrated interior transport (Figs. 1, 2, and 3). This net northward transport leaves the model's domain north of the Gulf Stream separation where it cools by the atmosphere, sinks, and returns southward as the North Atlantic Deep Water. An inert intermediate water is sandwiched between the northward flowing upper water ($\sigma_\theta < 26.8$) and the southward flowing NADW. The upper-ocean is continuously stratified and has a level of no motion corresponding to the densest isopycnal that surfaces; that is, all the fluid that is denser than the fluid associated with this isopycnal ($\sigma_\theta = 26.8$) is taken to be at rest.

This study is an extension of Nof's (1998) ''separation formula'' to the Atlantic Ocean. It enables one to obtain the net northward transport (of warm water) directly from the wind field and the latitude of the WBC separation. It shows that there must be some interhemispheric asymmetry in the wind field, the shape of the continents, or the cooling in order for a meridional transport of warm water to exist.

To illustrate this, we used three examples. First, we

considered an ocean 6000 km broad and showed that a net meridional transport is possible even when both the winds and continents are symmetrical and only the position of the WBC separation is asymmetrical due to high-latitude cooling (Fig. 4). For the second example we considered an ocean 5000 km broad extending from 40°S to 40°N where the two WBC separate again due to a combined wind–thermohaline influence. Here, however, the ocean is subject to no eastward wind stress along 40°N and to an eastward wind of 2 dyn cm^{-2} along 40°S. Our formula (2.12) shows that such an ocean will have a net meridional flow of 5 Sv. In the third example, we broadened the southern part of this hypothetical ocean from 5000 km to 10 000 km and considered symmetric winds along the eastern boundary. Under such conditions the transport is increased to 8 Sv. All three examples illustrate that it does not matter in which of the three processes (wind, high-latitude cooling, or the shape of the continents) there is asymmetry. However, the asymmetry must be quite severe for a significant interhemispheric transport of warm water to occur.

It should perhaps be stressed once more that, although the cooling by the atmosphere does not enter the problem explicitly, it enters the (no low and midlatitude upwelling) modeled process implicitly through the separation latitude, which adjusts to the amount of atmospheric cooling imposed in high latitudes. In other words, a change in the amount of atmospheric cooling and overturning rate will cause the (no-upwelling) modeled gyres to migrate meridionally until a new position [where (2.12) is again satisfied] is reached. Similarly, a change in the winds is, of course, not going to change the overturning rate. Instead, the modeled gyres will again shift their positions until (2.12) is once more satisfied. The analytical results were compared in detail to numerical simulations using MICOM and good agreement was found (Figs. 6 and 8).

The detailed application of the model to the Atlantic was obtained by integrating the momentum equations (using COAD data) along an open ''horseshoe'' path that begins at the separation point of the Brazil Current, proceeds counterclockwise along the eastern boundary, and ends at the separation of the Gulf Stream (Fig. 3). The transport derived in this fashion contains some of the Agulhas rings' mass flux, except the self-propelled transport (not included in the analytics and not resolved in the numerics), which is estimated to be no more than a few Sverdrups. Surprisingly, we found that the net northward warm water transport associated with this situation is less than 1 Sv! This is not because of the neglect of cooling but, rather, because the wind and high-latitude cooling (by the atmosphere) alone cannot drive any significant amount of *pure* warm upper water across the Atlantic equator.

As some analyses and numerical models have suggested, the Atlantic Intermediate Water must play a major role in the Atlantic meridional exchange. However, the way that the intermediate water enters the problem is not straightforward. Specifically, incorporation of upwelling (à la Goldsbrough 1933) into our model illustrates that any amount of intermediate water upwelled into the low and midlatitude Atlantic thermocline must be *equally split* between northward and southward fluxes. This implies that out of 20 Sv of intermediate water upwelled into the Atlantic thermocline, 10 Sv will be flowing northward beyond the Gulf Stream separation latitude and 10 Sv will be flowing southward and exit the South Atlantic via the Brazil Current (Figs. 10a,b).

Finally, it should be pointed out that our theory, which corresponds to an Atlantic with an open southern boundary, should be distinguished from the familiar numerical experiments that consider the Atlantic to be a closed box (e.g., Marotzke 1997). In our open model the upwelling in the Atlantic is forced by the dynamics whereas in the latter cases the upwelling in the Atlantic is due to the simple fact that the Atlantic is closed so that whatever sinks in the northeast must rise somewhere else within the box.

In summary, we can say (on the basis of the excellent agreement between the analytics and the numerics) that the (no upwelling) meridional transport of upper warm water in the Atlantic driven by both wind and high-latitude cooling can be adequately computed from the wind field and the observed separation latitudes of the western boundary currents [using (2.12)]. The calculation shows that this amount is small (<1 Sv) and that low and midlatitude upwelling of 20 Sv or so must take place somewhere within the limits of the Atlantic equatorward of the separation latitudes. The wind field and the high-latitude cooling then push half of this transport (10 Sv) toward the north and half toward the south.

It is hoped that these results will be examined with more detail in the future using more general numerical simulations. In particular, it is hoped that the implications of our model to the Indian and Pacific Oceans will be examined in detail. Our model implies that, in these oceans, there must be some conversion of both surface and deep water to intermediate water (see Fig. 10b). How (and if) this is achieved is not clear at this stage.

Acknowledgments. This study was supported by the National Science Foundation (NSF) under Contracts OCE 9633655 and OCE 9503816, National Aeronautics and Space Administration Grants NAGW 4883 and NAG5-4813, and Office of Naval Research Grant N00014-96-1-0541. Drawings were done by Beth Raynor.

REFERENCES

Arakawa, A., 1966: Computational design for long-term numerical integration of the equations of fluid motion. Two dimensional incompressible flow. Part 1. *J. Comput. Phys.*, **1**, 119–143.

Barnier, B., P. Marchesiello, A. P. de Miranda, J.-M. Molines, and M. Coulibaly, 1998: A sigma-coordinate primitive equation model for studying the circulation in the South Atlantic. Part I: Model

configuration with error estimates. *Deep-Sea Res. I,* **45**, 543–572.

Bennett, S. L., 1988: Where three oceans meet: The Agulhas retroflection region. Ph.D. thesis, MIT/WHOI, WHOI-88-51, xxvii + 367 pp. [Available from Massachusetts Institute of Technology, Cambridge, MA 02139.]

Bleck, R., and D. Boudra, 1981: Initial testing of a numerical ocean circulation model using a hybrid, quasi-isopycnic vertical coordinate. *J. Phys. Oceanogr.,* **11,** 755–770.

——, and ——, 1986: Wind-driven spin-up in eddy-resolving ocean models formulated in isopycnic and isobaric coordinates. *J. Geophys. Res.,* **91,** 7611–7621.

——, and L. Smith, 1990: A wind-driven isopycnic coordinate model of the north and equatorial Atlantic Ocean. Part I: Model development and supporting experiments. *J. Geophys. Res.,* **95,** 3273–3285.

Boris, J., and D. Book, 1973: Flux-corrected transport. I:SHASTA, a fluid transport algorithm that works. *J. Comput. Phys.,* **11,** 38–69.

Boudra, D. B., and E. P. Chassignet, 1988: Dynamics of Agulhas retroflection and ring formation in a numerical model. Part I: The vorticity balance. *J. Phys. Oceanogr.,* **18,** 280–303.

Byrne, D., A. Gordon, and W. Haxby, 1995: Agulhas eddies: A synoptic view using Geosat ERM data. *J. Phys. Oceanogr.,* **25,** 902–917.

Charney, J. G., 1955: The Gulf Stream as an inertial boundary layer. *Proc. Natl. Acad. Sci.,* **41,** 731–740.

Clement, A. C., and A. L. Gordon, 1995: The absolute velocity field of Agulhas eddies and the Benguela Current. *J. Geophys. Res.,* **100,** 22 591–22 601.

Dengg, J., 1993: The problem of Gulf Stream separation: A barotropic approach. *J. Phys. Oceanogr.,* **23,** 2182–2200.

Dewar, W. K., and C. Gailliard, 1994: The dynamics of barotropically dominated rings. *J. Phys. Oceanogr.,* **24,** 5–29.

Drijfhout, S. S., E. Maier-Reimer, and U. Mikolajewicz, 1996: Tracing the conveyor belt in the Hamburg large-scale geostrophic ocean general circulation model. *J. Geophys. Res.,* **101,** 22 563–22 575.

Duncombe Rae, C. M., S. L. Garzoli, and A. L. Gordon, 1996: The eddy field of the southeast Atlantic Ocean: A statistical census from the BEST project. *J. Geophys. Res.,* **101,** 11 949–11 964.

Ezer, T., and G. Mellor, 1992: A numerical study of the variability and the separation of the Gulf Stream, induced by surface atmospheric forcing and lateral boundary flows. *J. Phys. Oceanogr.,* **22,** 660–682.

Garzoli, S. L., A. L. Gordon, V. Kamenkovich, D. Pillsbury, and C. Duncombe-Rae, 1996: Variability and sources of the southeastern Atlantic circulation. *J. Mar. Res.,* **54,** 1039–1071.

——, G. J. Goñi, A. J. Mariano, and D. B. Olson, 1997: Monitoring the upper southeastern Atlantic transports using altimeter data. *J. Mar. Res.,* **55,** 453–481.

Goldsbrough, G. R., 1933: Ocean currents produced by evaporation and precipitation. *Proc. Roy. Soc. London,* **141A,** 512–517.

Goñi, G., S. Garzoli, A. Roubicek, D. Olson, and O. Brown, 1997: Agulhas ring dynamics from TOPEX/POSEIDON satellite altimeter data. *J. Mar. Res.,* **55,** 861–883.

Gordon, A. L., 1986: Inter-ocean exchange of thermocline water. *J. Geophys. Res.,* **91,** 5037–5050.

——, and W. F. Haxby, 1990: Agulhas eddies invade the South Atlantic: Evidence from Geosat altimeter and shipboard conductivity–temperature–depth survey. *J. Geophys. Res.,* **95,** 3117–3127.

——, J. R. E Lutjeharms, and M. L. Gründlingh, 1987: Stratification and circulaton at the Agulhas retroflection. *Deep-Sea Res.,* **34,** 565–599.

——, W. F. Ray, W. M. Smethie, and M. J. Warner, 1992: Thermocline and intermediate water communication between the South Atlantic and the Indian Oceans. *J. Geophys. Res.,* **97,** 7223–7240.

Hellerman, S., and M. Rosenstein, 1983: Normal monthly wind stress over the world ocean with error estimates. *J. Phys. Oceanogr.,* **13,** 1093–1104.

Hisard, P., C. Henin, R. Goughton, B. Piton, and P. Rual, 1986: Oceanic conditions in the tropical Atlantic during 1983 and 1984. *Nature,* **322,** 243–245.

Kamenkovich, V. M., Y. P. Leonov, D. A. Nechaev, D. A. Byrne, and A. L. Gordon, 1996: On the influence of bottom topography on the Agulhas eddy. *J. Phys. Oceanogr.,* **26,** 892–912.

Killworth, P. D., 1991: Cross-equatorial geostrophic adjustment. *J. Phys. Oceanogr.,* **21,** 1581–1601.

Kunze, E., and T. B. Sanford, 1996: Abyssal mixing: Where it is not. *J. Phys. Oceanogr.,* **26,** 2286–2296.

Lebedev, I., and D. Nof, 1996: The drifting confluence zone. *J. Phys. Oceanogr.,* **26,** 2429–2448.

Ledwell, J. R., A. J. Watson, and C. S. Law, 1993: Evidence for slow mixing across the pycnocline from an open-ocean tracer-release experiment. *Nature,* **364,** 701–703.

Levitus, S., 1982: *Climatological Atlas of the World Ocean.* NOAA Prof. Paper No. 13, U.S. Govt. Printing Office, Washington, DC, 173 pp.

Lueck, R. G., and T. D. Mudge, 1997: Topographically induced mixing around a shallow seamount. *Science,* **276,** 1831–1833.

Lutjeharms, J. R. E., 1988: Examples of extreme circulation events at the Agulhas retroflection. *S. Afr. J. Sci.,* **84,** 584–586.

——, and A. L. Gordon, 1987: Shedding of an Agulhas ring observed at sea. *Nature,* **325,** 138–140.

——, and H. R. Valentine, 1988: Eddies at the subtropical convergence south of Africa. *J. Phys. Oceanogr.,* **18,** 761–774.

——, and R. C. Van Ballegooyen, 1988: The retroflection of the Agulhas Current. *J. Phys. Oceanogr.,* **18,** 1570–1583.

Marchesiello, P., B. Barnier, and A. P. de Miranda, 1998: A sigma-coordinate primitive equation model for studying the circulation in the South Atlantic. Part II: Meridional transports and seasonal variability. *Deep-Sea Res. I,* **45,** 573–608.

Marotzke, J., 1997: Boundary mixing and the dynamics of three-dimensional thermohaline circulations. *J. Phys. Oceanogr.,* **27,** 1713–1728.

Matano, R. P., 1993: On the separation of the Brazil Current from the coast. *J. Phys. Oceanogr.,* **23,** 79–90.

——, and S. G. H. Philander, 1993: Heat and mass balances of the South Atlantic Ocean calculated from a numerical model. *J. Geophys. Res.,* **98,** 977–984.

McCartney, M. S., and M. E. Woodgate-Jones, 1991: A deep-reaching anticyclonic eddy in the subtropical gyre of the eastern South Atlantic. *Deep-Sea Res.,* **38,** S411–S443.

Myers, P., A. Fanning, and A. Weaver, 1996: JEBAR, bottom pressure torque, and Gulf Stream separation. *J. Phys. Oceanogr.,* **26,** 671–683.

Nelson, G., and L. Hutchings, 1983: The Benguela upwelling area. *Progress in Oceanography,* Vol. 12, Pergamon, 333–356.

Nof, D., 1981: On the β-induced movement of isolated baroclinic eddies. *J. Phys. Oceanogr.,* **11,** 1662–1672.

——, 1998: The ''separation formula'' and its application to the Pacific Ocean. *Deep-Sea Res. I,* **45,** 2011–2033.

Oberhuber, J. M., 1988: *The Budget of Heat, Buoyancy and Turbulent Kinetic Energy at the Surface of the Global Ocean.* Max-Planck-Institut für Meteorologie, Rep. No. 15, 19 pp. [Available from Max-Planck-Institut für Meteorologie, Bundesstraße 55, 20147 Hamburg, Germany.]

Olson, D. B., and R. H. Evans, 1986: Rings of the Agulhas Current. *Deep-Sea Res.,* **33,** 27–42.

Ou, H. W., and W. P. M. De Ruijter, 1986: Separation of an inertial boundary current from a curved coastline. *J. Phys. Oceanogr.,* **16,** 280–289.

Parsons, A. T., 1969: A two-layer model of Gulf Stream separation. *J. Fluid Mech.,* **39,** 511–528.

Peterson, R. G., and L. Stramma, 1991: Upper-level circulation in the South Atlantic Ocean. *Progress in Oceanography,* Vol. 26, Pergamon, 1–73.

Polzin, K. L., K. G. Speer, J. M. Toole, and R. W. Schmitt, 1996: Intense mixing of Antarctic Bottom Water in the equatorial Atlantic Ocean. *Nature,* **380,** 54–57.

——, J. M. Toole, J. R. Ledwell, and R. W. Schmitt, 1997: Spatial variability of turbulent mixing in the abyssal ocean. *Science,* **276,** 93–96.

Qiao, L., and R. H. Weisberg, 1997: The zonal momentum balance of the Equatorial Undercurrent in the central Pacific. *J. Phys. Oceanogr.,* **27,** 1094–1119.

Radko, T., 1997: Theoretical studies in mesoscale jets and vortices. Ph.D. dissertation, The Florida State University, 129 pp. [Available from Strozier Library, The Florida State University, Tallahassee, FL 32306.]

Rintoul, S. R., 1991: South Atlantic interbasin exchange. *J. Geophys. Res.,* **96,** 2675–2692.

Roemmich, D., 1983: The balance of geostrophic and Ekman transports in the tropical Atlantic Ocean. *J. Phys. Oceanogr.,* **13,** 1534–1539.

Saunders, P. M., and B. A. King, 1995: Oceanic fluxes on the WOCE A11 Section. *J. Phys. Oceanogr.,* **25,** 1942–1958.

Schlitzer, R., 1996: Mass and heat transports in the South Atlantic derived from historical hydrographic data. *The South Atlantic: Present and Past Circulation,* G. Wefer, Ed., Elsevier, 15 pp.

Schmitz, W. J., Jr., 1996: On the world ocean circulation. Vol. 1, Some global features/North Atlantic circulation. Woods Hole Oceanographic Institution Tech. Rep., WHOI-96-03. [Available from Woods Hole Oceanographic Institution, Woods Hole, MA 02543.]

Semtner, A. J., and R. M. Chervin, 1988: A simulation of the global ocean circulation with resolved eddies. *J. Geophys. Res.,* **93,** 15 502–15 522.

Shannon, L. V., 1985: The Benguela ecosystem. I. Evolution of the Benguela, physical features and processes. *Oceanography and Marine Biology: An Annual Review,* M. Barnes, Ed., Vol. 23, University Press, 105–182.

Speer, K. G., J. Holfort, T. Reynaud, and G. Siedler, 1996: South Atlantic Heat Transport at 11°S. *The South Atlantic: Present and Past Circulation,* G. Wefer, W. Berger, G. Siedler, and D. Webb, Eds., Springer-Verlag, 105–120.

Stramma, L., and R. J. Peterson, 1990: The South Atlantic Current. *J. Phys. Oceanogr.,* **20,** 846–859.

Thompson, J. D., and W. J. Schmitz Jr., 1989: A limited-area model of the Gulf Stream: Design, initial experiments, and model-data intercomparison. *J. Phys. Oceanogr.,* **19,** 791–814.

Toole, J. M., K. L. Polzin, and R. W. Schmitt, 1994: Estimates of diapycnal mixing in the abyssal ocean. *Science,* **264,** 1120–1123.

van Ballegooyen, R. C., M. L. Gründlingh, and J. R. E. Lutjeharms, 1994: Eddy fluxes of heat and salt from the southwest Indian Ocean into the southeast Atlantic Ocean: A case study. *J. Geophys. Res.,* **99,** 14 053–14 070.

Veronis, G., 1973: Model of World Ocean circulation. Part I: Wind-driven, two layer. *J. Mar. Res.,* **31,** 228–288.

——, 1976: Model of World Ocean circulation. Part II: Thermally driven, two-layer. *J. Mar. Res.,* **34,** 199–216.

Whitworth, T., III, and W. D. Nowlin Jr., 1987: Water masses and currents of the southern ocean at the Greenwich Meridian. *J. Geophys. Res.,* **92,** 6462–6476.

Woodruff, S. D., R. J. Slutz, R. L. Jenne, and P. M. Steurer, 1987: A comprehensive ocean–atmosphere data set. *Bull. Amer. Meteor. Soc.,* **68,** 1239–1250.

Zalesak, S. T., 1979: Fully multidimensional flux-corrected transport algorithms for fluids. *J. Comput. Phys.,* **31,** 335–362.